GEOLOGICA BELGICA (2003) 6/1-2: 3-23

KARST-METEORIC DEDOLOMITIZATION IN JURASSIC CARBONATES, LEBANON

Fadi H. NADER[1*], Rudy SWENNEN[1] & Raoul OTTENBURGS[1]

(14 figures, 1 table)

1. Katholieke Universiteit Leuven, Afd. Fysico-chemische Geologie, Celestijnenlaan 200C, B-3001 Heverlee, Belgium. Fadi.Nader@geo.kuleuven.ac.be

* *Lebanese National Council for Scientific Research scholar.*

ABSTRACT. This study shows that dedolomites may indicate emergence and karst meteoric diagenesis, providing invaluable information about the original dolomite rock and the calcitizing fluids. The relative increase of permeability in dolomitized zones (called 'pockets') within the limestone rock-mass of the Lebanese Jurassic Kesrouane Formation is believed to have played an important role in enhancing dedolomitization through preferential circulation of karst-meteoric waters in these pockets. Nonstoichiometry of the original dolomites (expressed by mole % $CaCO_3$) appears to be a major driving factor for dedolomitization, while clay content seems to protect the nonstoichiometric dolomites from becoming dedolomites. The calcitizing fluids were fresh oxidizing waters circulating in an open system - typical of karst aquifers. During dedolomitization, Sr, Fe and Mn were released from the pre-existing dolomite minerals without being incorporated in the precipitating calcite. The $\delta^{13}C$ values of the dedolomites supports meteoric diagenesis with contribution of soil derived carbon (values ranging from -2.40 to -2.32 ‰ PDB), while the 'meteoric calcite line' provides a clue to estimate the $\delta^{18}O$ value of the dedolomitizing fluid.

KEYWORDS: Lebanon, carbonate, dedolomite, stoichiometry, stable isotope, meteoric calcite line.

1. Introduction

Von Morolot (1847) was the first to use the term 'dedolomite', describing dolomite that was replaced by calcite during near-surface chemical weathering (in Back *et al.*, 1983). He suggested that dedolomitization is mainly due to the sulphate ions which were derived from the dissolution of gypsum or anhydrite:

$$CaSO_4 + CaMg(CO_3)_2 \rightarrow 2CaCO_3 + MgSO_4$$

More than a century later, dedolomitization became, according to Al-Hashimi and Hemingway (1973), an "important stage in carbonate diagenesis". This is also reflected by a broad wave of publications, most of which were released in the late 1960s (e.g. Evamy, 1963, 1967; Katz, 1968, 1971; Folkman, 1969). Folkman (1969) suggested that the sulfate ions, needed for von Morolot's reaction, might come from the oxidation of pyrite, and not necessarily from gypsum dissolution. Meanwhile, the restriction of the mechanism to the dolomite-calcium sulfate reaction became outdated (Katz, 1968, 1971; Al-Hashimi & Hemingway, 1973). Back *et al.* (1983) proposed a mechanism that properly explains the mineralogical and geochemical process of dedolomitization in typical carbonate aquifers. Their work is based on field and theoretical investigations combined with mass-balance calculations.

Several papers reported dedolomite occurrences in a wide range of diagenetic environments, although the majority of the case studies describe near-surface dedolomitization (through meteoric flushing, either in a karstic aquifer or below an erosional unconformity; e.g. Goldberg, 1967; Braun & Friedman, 1970; Al-Hashimi & Hemingway, 1973). Wood & Armstrong (1975) (in Budai *et al.*, 1984) attributed some dedolomite to contact metamorphism. Longman & Mench (1978) associated dedolomitization to fresh-water, while Land & Prezbindowsky (1981) to hot calcium-rich brine migration in a dolomitic reservoir. Magaritz & Kafri (1981) described another type of dedolomite produced by mixing marine and meteoric waters. More recently, burial dedolomitization has attracted some attention (e.g. Budai *et al.*, 1984; Kyung & Moore, 1996). Ronchi *et al.* (2000) discussed dedolomitization resulting from the influx of fresh meteoric water into a deeply buried dolomite reservoir.

Compilation of published data on dedolomite indicates that information on the dedolomitization process can be deduced from relict dolomite phases and the newly formed calcite. In most dedolomitized rocks, the origi-

nal dolomite is partially preserved. If not completely altered, these relict phases can provide invaluable information about the original dolomite. The produced calcite may hold some clues about the related fluids and the conditions of formation. This paper aims to demonstrate that careful investigations of dedolomites may reveal substantial data concerning the diagenetic conditions that occurred during karst-related dedolomitization. Results presented in this paper can be of use to recognize features indicative for emergence.

2. Geological setting

Lebanon is located along the eastern coast of the Mediterranean Sea (Fig. 1A). Its general morphology consists of two mountain chains (Lebanon and Anti-Lebanon) separated by a high plain (the Bekaa; Fig. 1B). Both ranges trend almost NNE-SSW. To the West, Mount Lebanon borders the Mediterranean Sea with steep slopes and includes the highest altitude in its northern part (i.e. Qornet es Saouda, 3083 m). This mountain chain is limited to the East by the Yammouneh Fault (Fig. 1C), a segment of the Dead Sea Transform Fault, which constitutes the boundary between the Arabian plate and the Levant microplate. It extends from the Gulf of Aqaba in Jordan to the Taurus mountains in Turkey (Fig. 1A). The tectonics of the Middle East region and the existing seismic activity are current research topics (e.g. Beydoun, 1988; Butler *et al.*, 1997, 1998; Seber *et al.*, 1997; Butler & Spencer, 1999; Griffiths *et al.*, 2000; Brew *et al.*, 2001; Gomez *et al.*, 2001).

The stratigraphy of Lebanon has been investigated by a number of authors (e.g. Dubertret, 1955; Saint-Marc, 1974, 1980; Walley, 1983, 1997; Beydoun, 1988; Fig. 2). Several other studies were carried out mainly on detailed stratigraphy and petrology of particular regions and/or geological formations (Ja'ouni, 1971; Abu-Shushah, 1976; Noujeim, 1977). Recently, Abdel-Rahman & Nader (2002) discussed the general petrographic and geochemical characteristics of the Jurassic-Cretaceous carbonates of central Lebanon.

The Lebanese Jurassic carbonate platform is part of the more extensive Palmyride basin (stretching from present day north-western Iraq to north-eastern Egypt through Syria and Lebanon). In Lebanon, the Jurassic rocks constitute the cores of the two mountain chains. In central and northern Mount-Lebanon, these strata have a total thickness exceeding 1600 m and mainly consist of dolomite and micritic limestone. The Late Jurassic is characterized by a period of regional uplift, emergence and erosion. Upon emergence, the Jurassic rock-mass was deeply fractured and karstified before volcanism took place (i.e. Bhannes Formation; Fig. 2). Subsequently, volcanic deposits and continental debris filled up the pre-existing fractures and depressions accentuating the paleotopography (Renouard, 1955).

The Kesrouane Formation (stratigraphic thickness exceeding 1000 m; Fig. 2) represents most of the Jurassic strata in Lebanon. This unit is characterized by a dolomitic basal sub-unit (informally called the Chouane Member) overlain by micritic limestone (typical of the Jurassic strata in Lebanon reflecting shallow marine depositional settings). In addition, pervasive replacement dolomitization randomly occurs within the whole sequence. Different models have been proposed to explain dolomites of similar stratigraphic age in Israel. Goldberg & Bogoch (1978) suggested a two-stage dolomitization process with an incipient stage occurring in a pelmicrite mud, probably before its lithification and in the original marine environment. The second stage is characterized by the obliteration of the pelletal structures and the growth of the dolomite cement rims, in fluids having different physico-chemical conditions. Buchbinder (1981) argues that dolomitization was post-depositional due to subsurface circulation of fluids either in a seawater-freshwater mixing zone or by warm subsurface brines.

3. Study area

The study area is located in central Lebanon, in the vicinity of Jiita town (Fig. 1C). This region includes a broad exposure of Jurassic rocks intensively cut by mostly east-west trending faults; most of which are pre-Cretaceous in age and have been reactivated during and/or after Cretaceous times. The western limit of the Jurassic outcrop is marked by a flexure, i.e. the "Lebanon Western Flexure". To the west of this hinge line, the various Cretaceous rock formations dip steeply towards the Mediterranean Sea. Within the study area, the Nahr el Kelb is the major river trending East-West with an approximate length of 30 km. The second most important hydrogeological feature is the underground network of the Jiita cave, which totals 9 km approximately. The cave hosts an underground river that is believed to be one of the major collectors of the Jurassic karstic aquifer in Mount Lebanon. The inland-extremity of the cave, where the source of the underground river is located, is accessed via a tunnel that was dug in 1971 on the northern side of Ouadi Daraya (Nahr el Kelb river). This is a 535 m long tunnel, dipping 21° downward and oriented South-North (from the entrance to the cave). It offers a remarkable geological section across the various horizontal strata of the lower part of the Kesrouane Formation (Fig. 3). The investigated dedolomites, which are the subject of this study, were collected inside this tunnel.

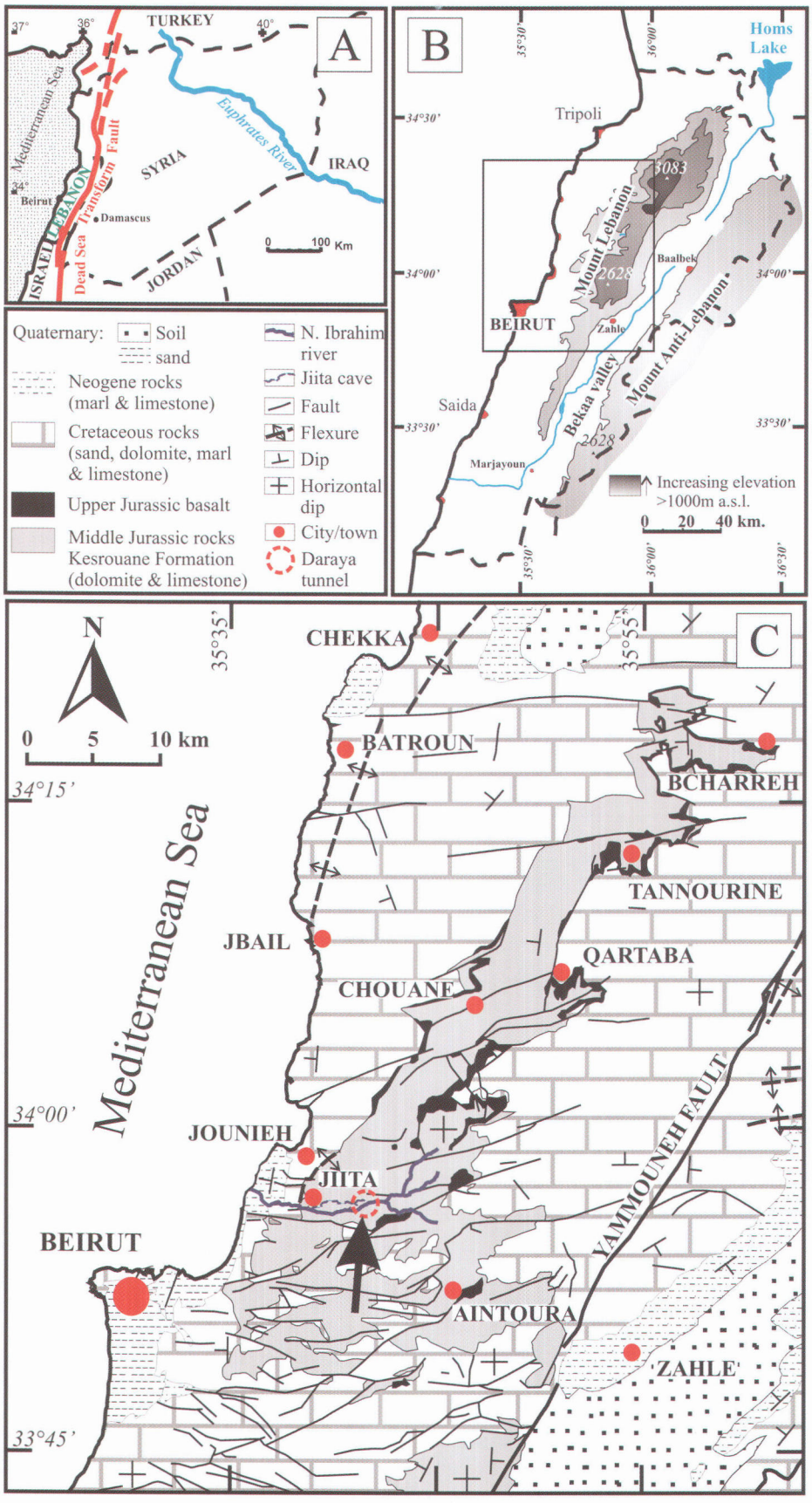

Figure 1. Location maps of the study area: (A) index-map showing a part of the Middle-East region and the Dead Sea Rift; (B) simplified topographic map of Lebanon with the rectangle corresponding to the area shown in (C); and (C) geological map of central northern Mount Lebanon (from Dubertret, 1955). The Daraya tunnel (site of the present study) is indicated with an arrow.

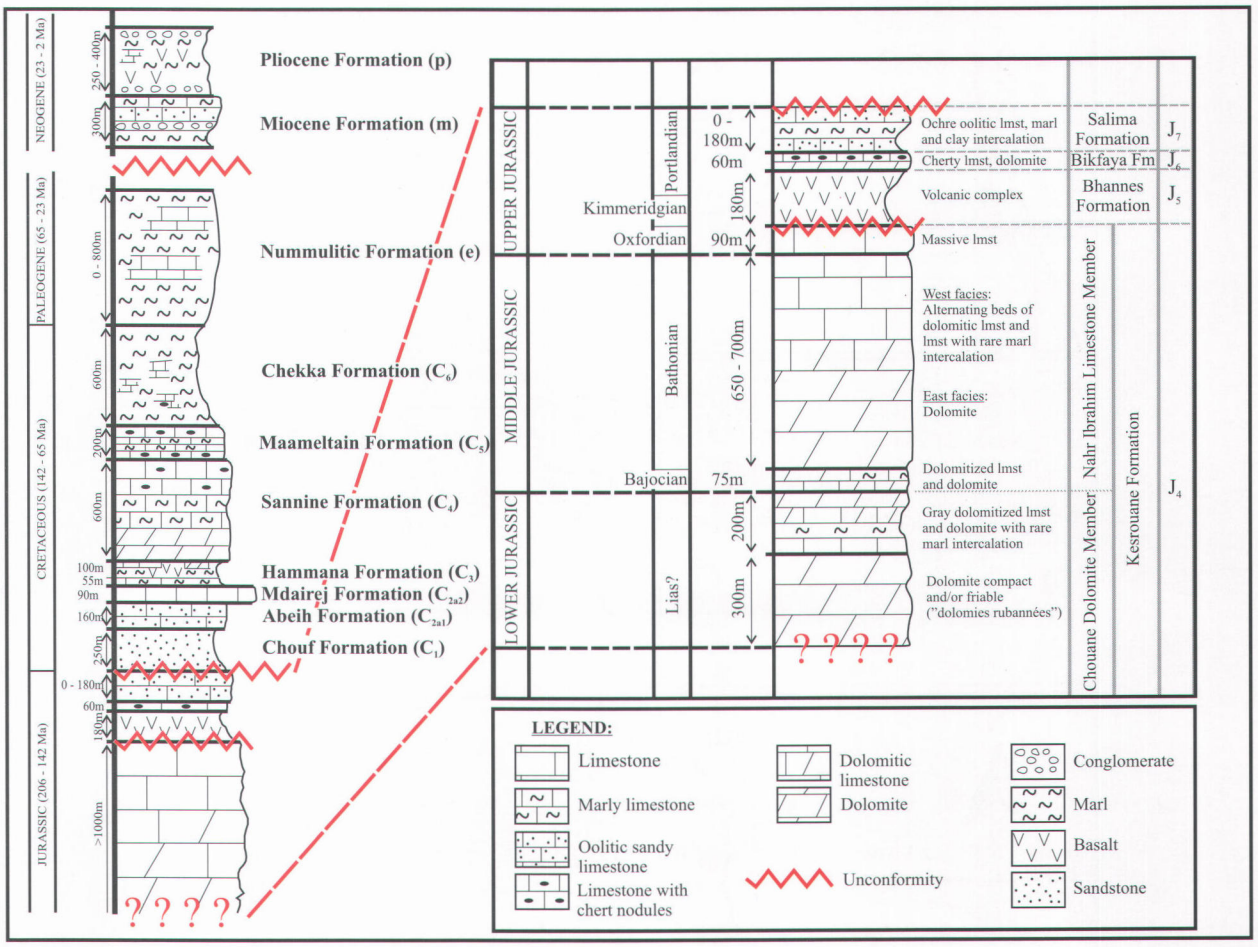

Figure 2. Simplified litho-stratigraphical log of the Lebanese Jurassic-Neogene rock sequence. The stratigraphy of the Jurassic segment, especially the Kesrouane Formation, is represented in detail (Renouard, 1951, 1955; Dubertret, 1955; Walley, 1997).

4. Methods

About 100 samples were drilled out of the walls of the Daraya tunnel; 20 of which were located within the dedolomite horizon. These samples were subjected to petrographic observations including conventional and cathodoluminescence microscopy (Technosyn Cold Cathodoluminescence Model 8200 Mark II; operation conditions were 16-20 kV gun potential, 420-600 µA beam current, 0.05 Torr vacuum and 5 mm beam width). Subsequently, various diagenetic phases were micro-sampled for measuring their carbon and oxygen stable isotopic composition. Analyses were done at the University of Erlangen – Germany (Institute of Geology and Mineralogy; Dr. M. Joachimsky). The carbonate powders were reacted with 100% phosphoric acid (density > 1.9; Wachter & Hayes, 1985) at 75°C in an online carbonate preparation line (Carbo-Kiel - single sample acid bath) connected to a Finnigan Mat 252 mass-spectrometer. All values are reported in per mil relative to V-PDB by assigning a $\delta^{13}C$ value of +1.95‰ and a $\delta^{18}O$ value of - 2.20‰ to NBS19. Oxygen isotopic compositions of dolomites were corrected using the fractionation factors given by Rosenbaum & Sheppard (1986). Reproducibility based on replicate analysis of laboratory standards is better than ±0.02‰ for $\delta^{13}C$ and ±0.03‰ for $\delta^{18}O$.

Pieces of representative samples were crushed and powdered before mineralogical analysis by X-ray diffraction (XRD) using a Phillips PW3710 unit with rotating sample-holder and secondary monochromator. Cu-Kα radiation (45 kV, 30 mA) was used and silicon was chosen as an internal standard. Dolomite nonstoichiometry (M% $CaCO_3$) was calculated using the relationship between calcium content and $d_{[104]}$ spacing (Goldsmith & Graf, 1958) and applying the equation of Lumsden to the measured $d_{[104]}$ spacing (Lumsden, 1979). Samples containing only calcite or dolomite were then leached in 20 ml 1 M HCl. After complete reaction the dissolved samples were evaporated. The residues were dissolved for a second time in 20 ml 1 M HCl. After filtration and dilution, Ca, Mg, Sr, Na, Fe, Mn and K were analyzed by flame atomic absorption spectrometry (AAS). Samples with both calcite and dolomite were subjected to a sequential separation procedure modified from Burns & Baker (1987) before AAS analyses. Removing the calcite phase was done

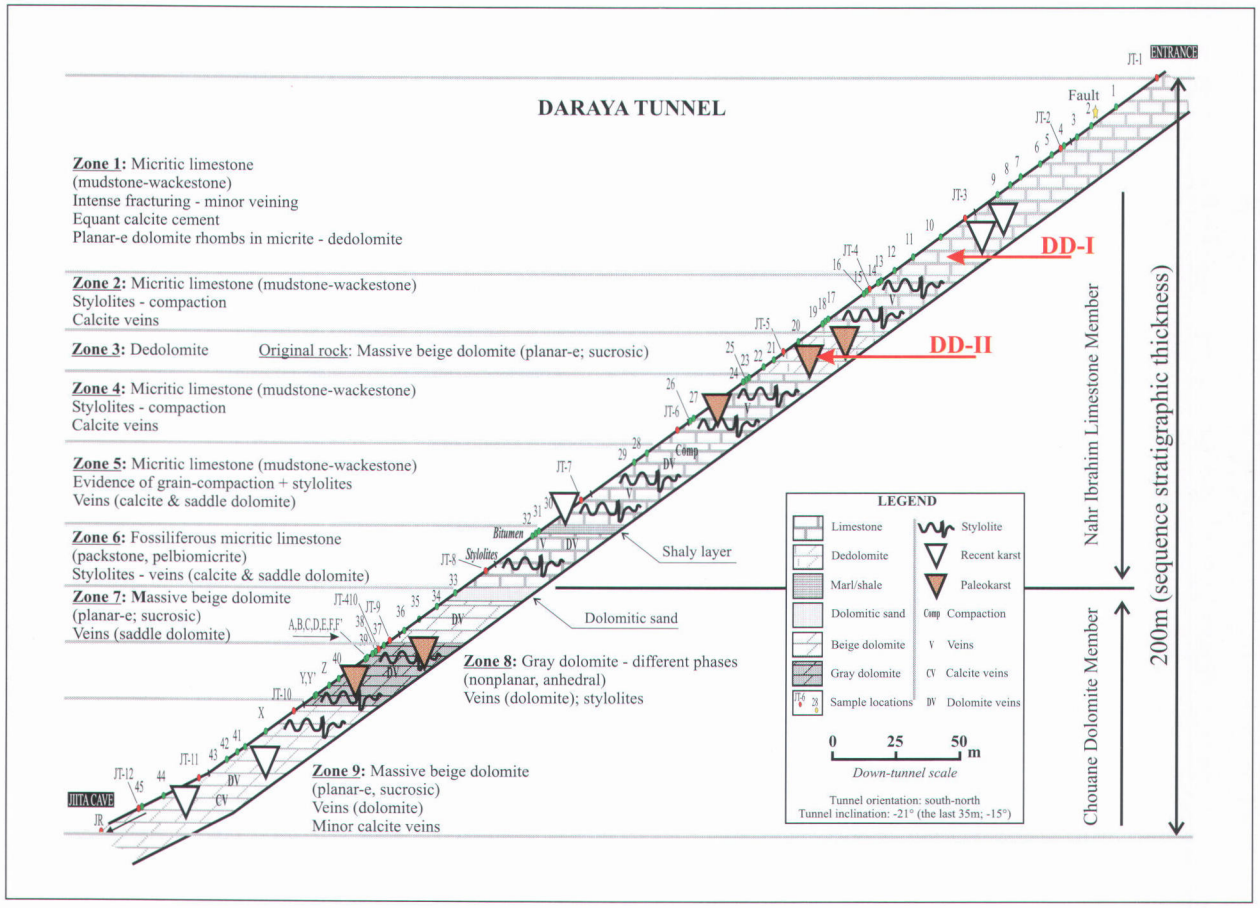

Figure 3. Geological cross-section along the Daraya tunnel (21° dipping downward; S-N orientation; leading to the terminal siphon of the Jiita cave). Almost all intercepted strata are horizontally bedded. The general lithology is represented by 9 distinct zones. The section also shows the positions of the dedolomites, the beige and the gray dolomites, as well as the various observed sites of karstification. The sampling locations are also included.

by leaching and shaking the samples in acetic acid buffered with ammonium acetate (pH = 5) for 5 hours. After filtering and rinsing, the resulting solution is considered to contain only the calcite phase while the remaining solids (assumed to represent the dolomite phase) were subjected to similar leaching procedures as described above for mono-phase samples. Analytical precision was generally better than 10 % at the 95% confidence level.

5. Petrography

The strata exposed in the Daraya tunnel represents a 200 m thick stratigraphic sequence - subdivided into 9 distinct zones according to lithological characteristics (Fig. 3). The upper 6 zones mainly consist of micritic limestone (dominantly mudstone - wackestone). The remaining zones feature two main types of dolomite rocks, the petrography of which is described below. Two distinct horizons of dedolomitized rocks were found in two previously dolomitized pockets within the limestone rocks (DD-I and DD-II; Fig. 3). These are located within a distance of 125 m along the tunnel (i.e. 45 m of stratigraphical thickness). The outcropping surfaces of each type (DD-I and DD-II) are very difficult to assess (i.e., the features are widely variable and difficult to detect with the naked eye).

5.1. Original rock: limestone

All the observed limestones are mudstones-to-wackestones suggesting that the depositional environment was shallow subtidal. This is also supported by the presence of isopachous cement around grains (replacing the earlier acicular cement), and curvilinear micro-fractures filled with very early marine cement. The latter are probably the result of synsedimentary tectonic displacement or initial compaction dewatering. Equant calcite cement in fossil molds (e.g. corals) are believed to represent early meteoric diagenesis which has led to the dissolution of aragonitic fossils prior to the precipitation of calcite. The observed drusy mozaic fabrics and the syntaxial overgrowth cements (especially around crinoids) may suggest continuous shallow burial under meteoric phreatic conditions. In the lower part of the exposed limestone sequence inside the tunnel,

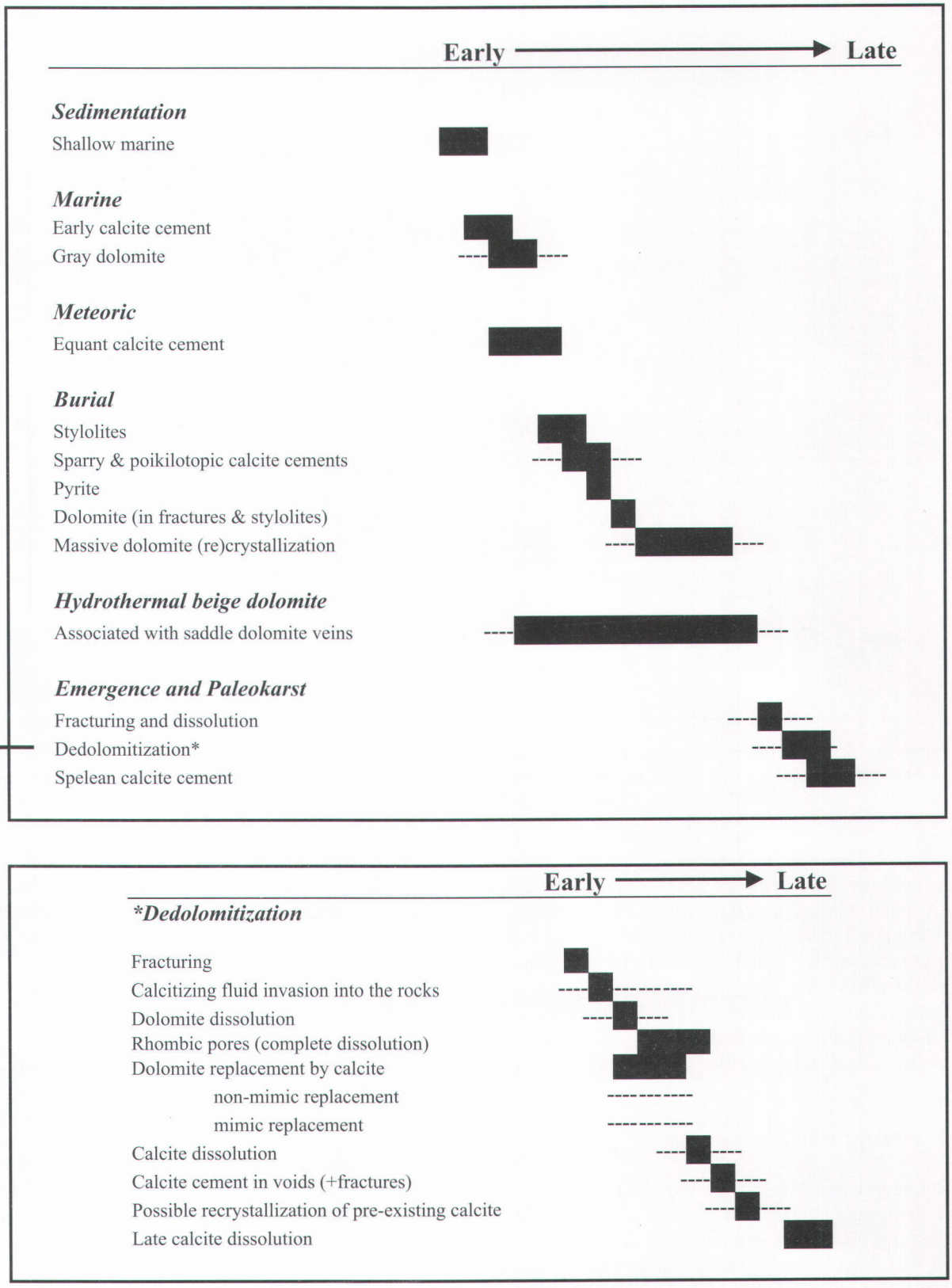

Figure 4. Sequence of diagenetic stages in the Jurassic carbonates exposed along the Daraya tunnel (Kesrouane Formation). The paragenesis of the dedolomitized rocks is presented in detail, separately.

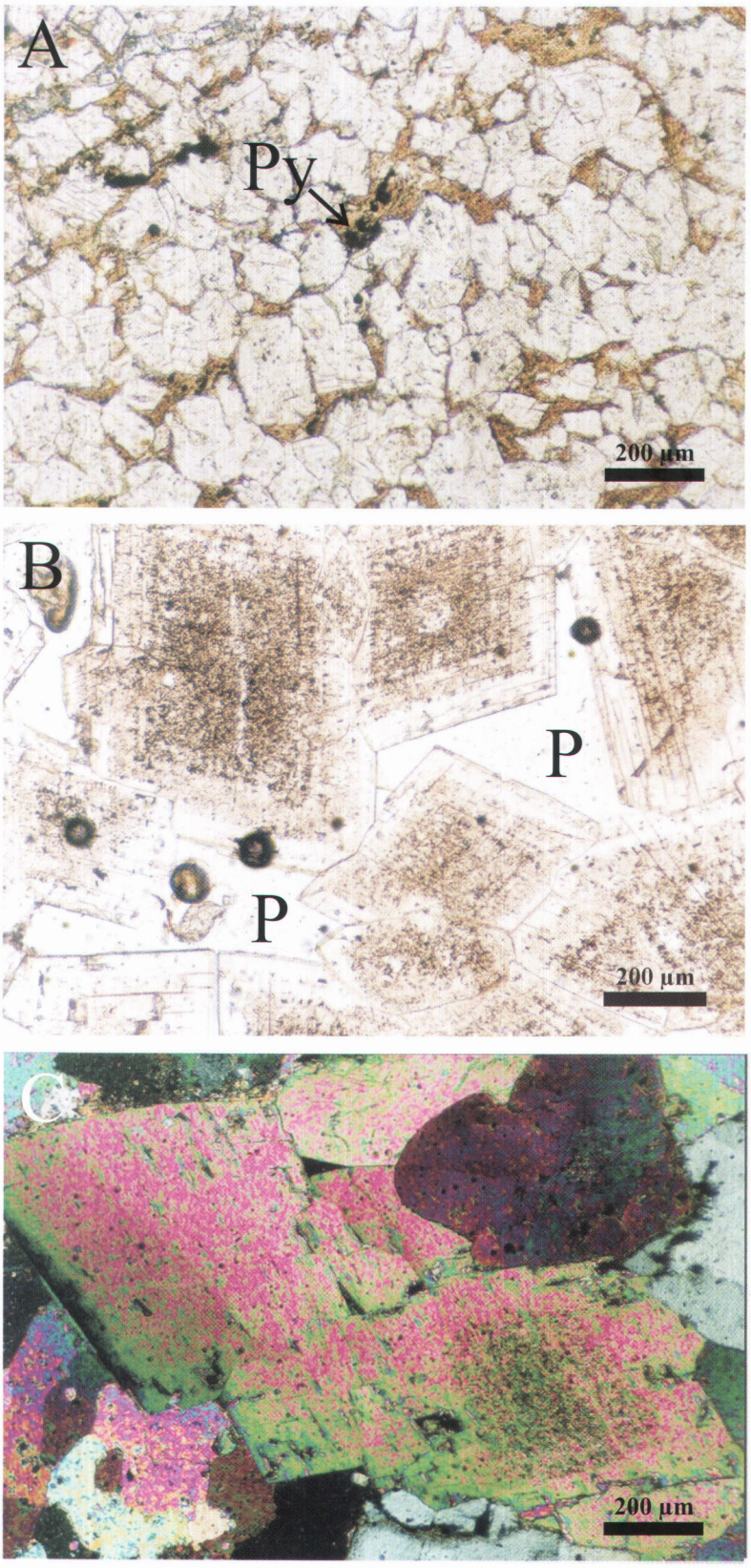

Figure 5. Transmitted light photomicrographs of gray dolomite (A), beige dolomite (B), and preserved dolomite from the dedolomitized horizons ('pockets'; crossed polars; C). Note the planar texture in the latter dolomites (B, C) compared to the non-planar crystals characterizing the gray dolomite. The 'pocket' dolomite exhibits sweeping extinction typical of saddle dolomite. Py is pyrite and P is porosity.

compaction stylolites were found. These could be markers of increased overburden pressure due to burial. Sparry calcite and poikilotopic cements (which characterize the lower-most zones) also suggest burial diagenesis in a presumed phreatic environment. The paragenetic evolution is presented in Fig. 4.

5.2. Original rock: dolomite

Two distinct types of dolomites were observed in the Daraya Tunnel (zones 7 to 9; Fig. 3). The first type is gray in hand specimen. It is composed of anhedral dolomite crystals, with sizes not exceeding 400 μm (Fig. 5A). They have a polymodal nonplanar texture. The local occurrence of evaporitic-like nodules within these rocks and the fact that they are stratigraphically bound (they are not found above zone 7 in Fig. 3) suggest early dolomitization in shallow marine lagoonal settings. The rock texture displays iron-oxides, pyrite, clay and organic matter between the dolomite crystals.

The second dolomite type is beige in hand specimen. Microscopically, it consists of subhedral to euhedral dolomite crystals with an average size exceeding 400 μm (Fig. 5B). These show cloudy centers surrounded by clear cement rims and generally show undulatory extinction typical of saddle dolomite. The crystals have a unimodal, planar-e texture typical of sucrosic dolomite (see Sibley & Gregg, 1987). The beige dolomites are not stratigraphically-bound and occur also as scattered pockets in the overlying limestone strata. These dolomites exhibit a 'clean' structure with relatively coarse-crystalline texture and high intercrystalline porosity (Fig. 5C). Although, all types of dolomites exhibit a general molted red cathodoluminescence pattern, the beige dolomite crystals that align pores show alternating luminescence patterns witnessing several distinct layers of dolomite cement. Field observation of beige dolomite occurrences associated with volcanic rocks and the nature of the crystals (i.e. saddle dolomites) may point towards rapid dolomitization by means of hydrothermal activity (cf. Searl, 1989).

5.3. Dedolomite

Two distinct dedolomitized horizons (DD-I and DD-II) were recognized in the Daraya sequence (Fig. 3). The occurrence of both horizons coincides with clear paleokarst features, such as dissolution conduits entirely filled up with red-brown soil (Fig. 6A). Recent karst is

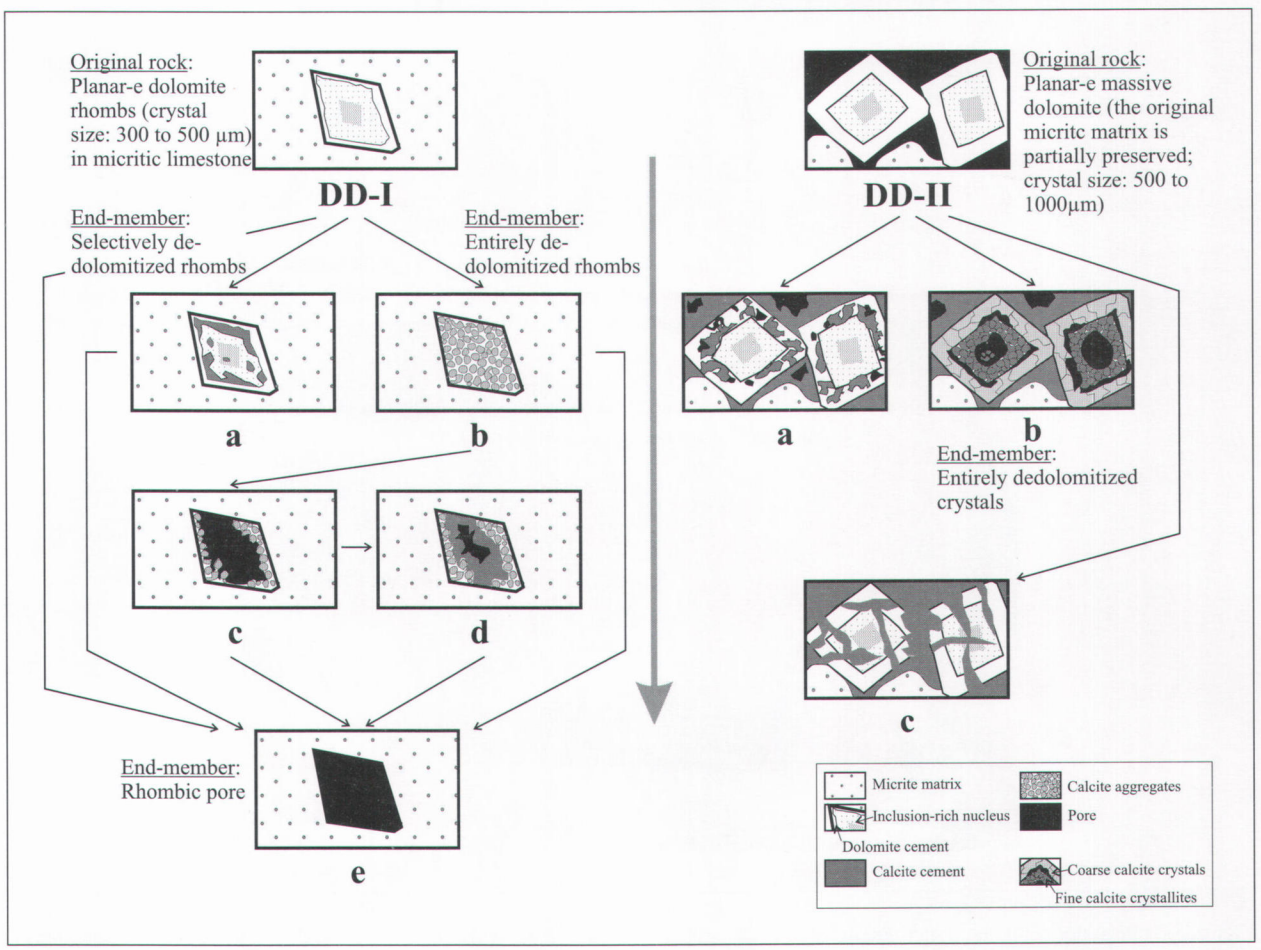

Figure 7. Types of dedolomite fabrics based on the texture of the original rock (more explanation is given in text).

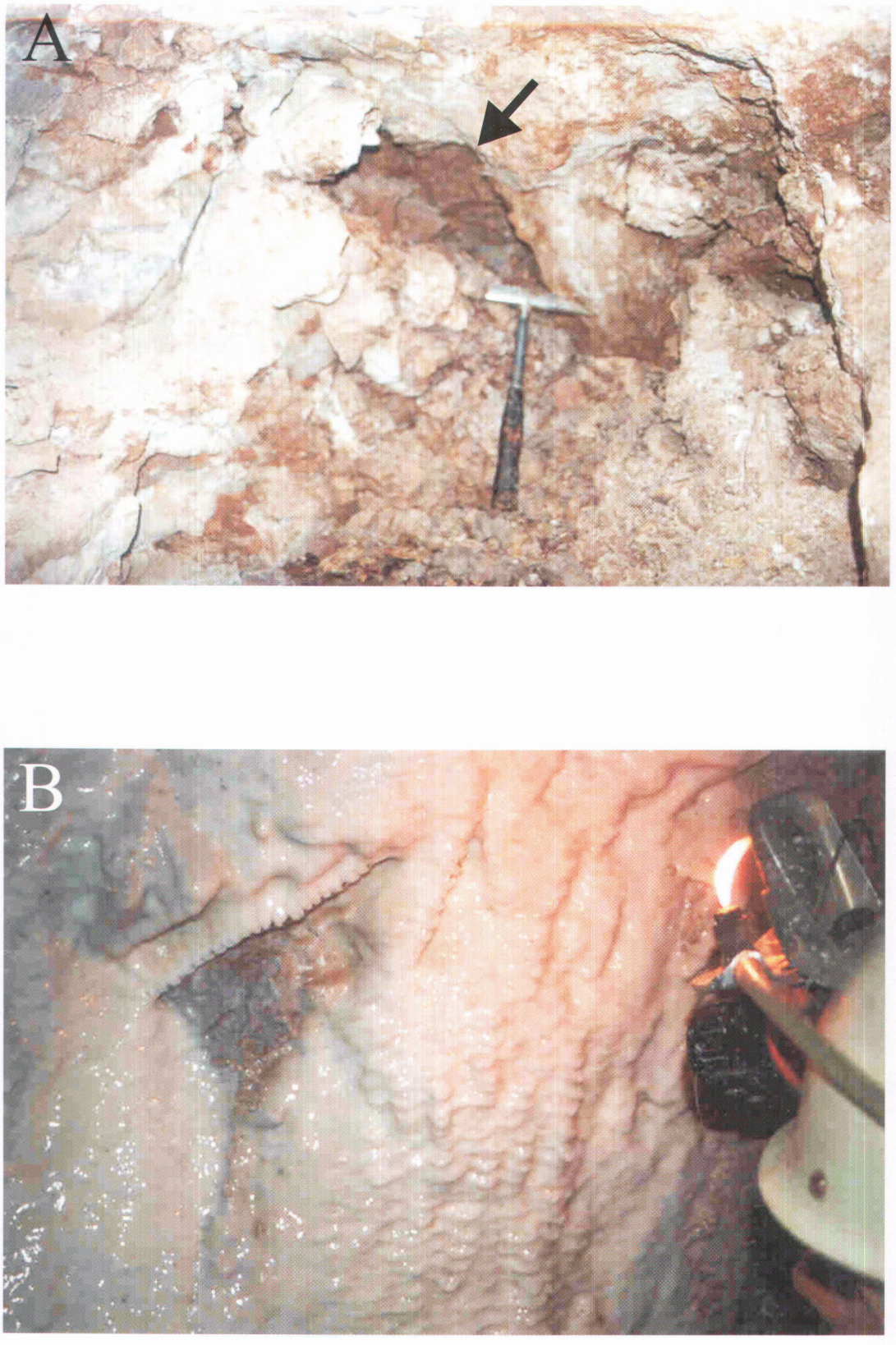

Figure 6. Photographs showing paleokarst (A) and present-day karst (B) features inside the Daraya tunnel. The former shows no 'present-day' water dripping and consists of ancient dissolution conduits and cracks occluded by red-brown paleo-soil (indicated by an arrow). Some of the recent karst features post-date the tunnel and include various types of speleothems (B).

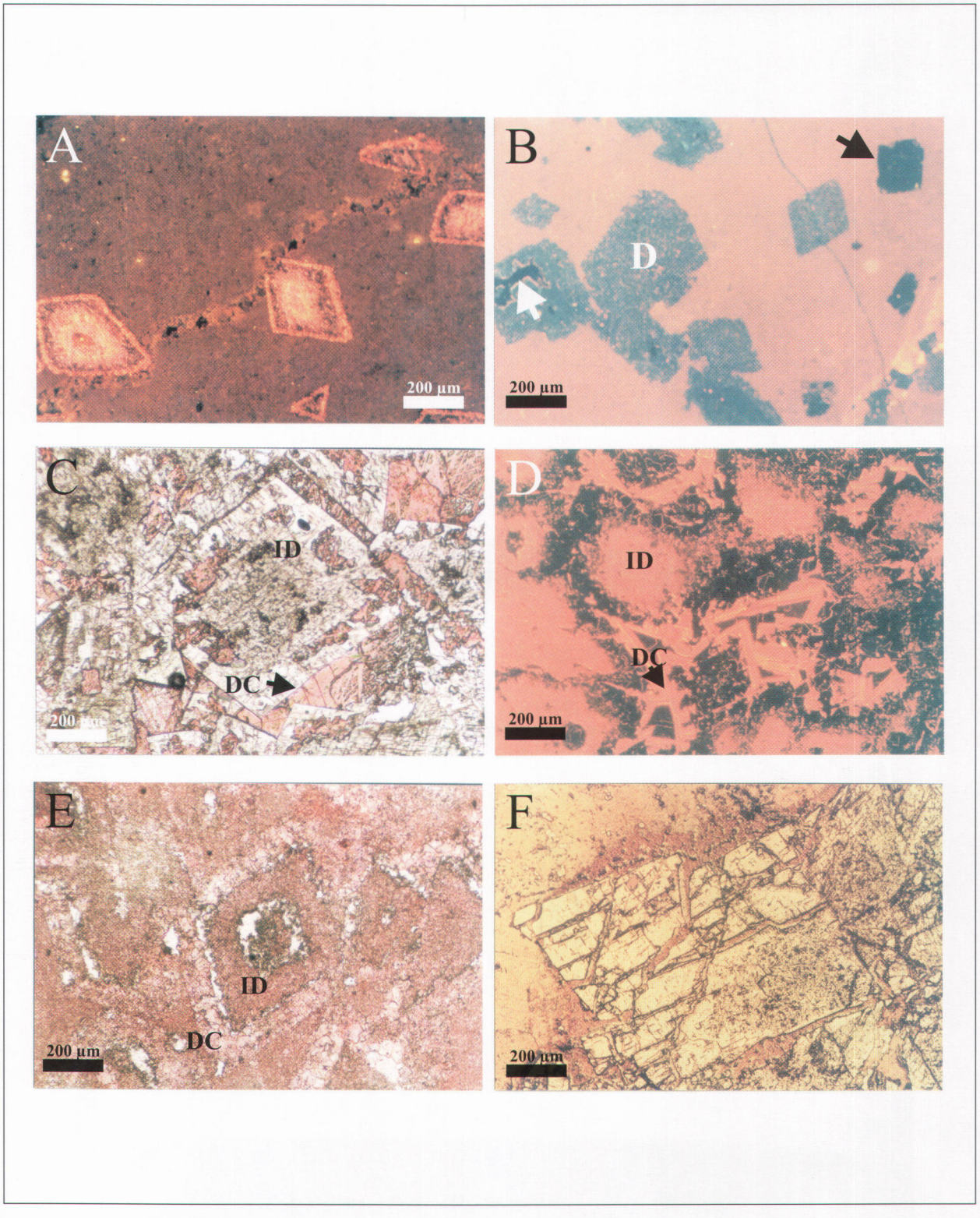

Figure 8. Transmitted light and CL photomicrographs of the different dedolomite textures: (A) Partial selective dissolution along the interface between core and outer rims of the original dolomite (non-luminescent zone inside the dolomite rhombs; typical of DD-Ia fabric); (B) complete calcitization of the dolomite crystals by non-luminescent calcite crystallites [D] - DD-Ib – and/or dissolution (white arrow: DD-Id; black arrow: DD-Ie); (C) photomicrograph of a stained thin section showing calcite cement partially occluding dissolution-voids at the interior of the dolomite rhomb [ID] – [DC] is the dolomite cement rims (DD-IIa); (D) CL-patterns of DD-IIa, calcite is non luminescent, while dolomite phases show dull red-orange luminescence (ID: dolomite core; DC: dolomite rims); (E) completely dedolomitized rhomb (DD-IIb) – calcite mimic the original dolomite phases [ID and DC] and selective dissolution is observed in the nucleus and at the ID/DC interface; (F) Dolomite showing slight dedolomitization, the crystals are fragmented and then corroded as a result of tectonic deformation followed by calcite invasion (DD-IIc).

also observed, and some speleothems were formed after the excavation of the tunnel (Fig. 6B). Such karstification consists of open dissolution conduits and different types of speleothems (e.g. dripstones, stalactites). Contrary to the paleokarst features, these show 'present-day' water seepage.

DD-I is creamy beige in hand specimen. It consists of euhedral dedolomite crystals (dolomite pseudomorphs), with an average size in the order of 400 μm, in a micritic limestone matrix. Fractures and veins with calcite infilling are also present in the matrix. The rhombs have a unimodal planar-e texture and lack undulatory extinction, they constitute approximately 25% of the matrix. Further petrographic investigation of these rhombs resulted in distinguishing 5 different dedolomite fabrics (Fig. 7).

DD-Ia represents dedolomite rhombs with selective calcite replacement or cement along the interface between the cores and the cement-rims of the original dolomite crystals. Some of these rhombs show calcite replacement/cement inside their cores as well. Under CL, the crystals show clear crystal zoning reflecting the different mineral-phases (dolomite/calcite) and the original dolomite zoning resulting from changes in the water chemistry (Grover & Read, 1983; Barnaby & Rimstedt, 1989; Machel, 2000). The calcite inside the rhombs is non-luminescent, while the dolomite shows dull-bright-dull-luminescence patterns (from crystal-core to rims; Fig. 8A). DD-Ib consists of calcite with a crystallite texture (calcite crystals are < 50 μm in size); the original rhombic outline is still preserved. These calcite infills are non-luminescent (Fig. 8B). DD-Ic has the same attributes as DD-Ib, but it was subjected to dissolution. If the dissolution completely removes the calcite crystallites and/or the original dolomite, a rhombic mold is produced (DD-Ie; Fig. 8B). If dissolution is partial, the empty space might get filled up with transparent calcite cement, the crystal size of which ranging between 50 and 100 μm (DD-Id). The discussed fabrics reveal obvious dedolomitization trends with three main end-members: 1) DD-Ia, a particular case of selective dedolomitization along original crystalline internal structure; 2) DD-Ib, completely dedolomitized rhombs; and 3) DD-Ie, rhombic pores (products of complete dissolution of the dedolomite fabrics and the original dolomite rhombs).

DD-II is dark beige to brown in hand specimen. It consists of subhedral to euhedral calcitized dolomite crystals with sizes ranging between 500 and 1000 μm. These have a unimodal planar-e texture. The rock texture shows intensive structural deformation through the mechanical fragmentation of the dolomite rhombs and the twinning of the calcite cement, which might relate to tectonic deformation during uplift (Upper-Jurassic and Neogene). Most of the remaining dolomite rhombs exhibit cloudy centers surrounded by clear rims.

Fig. 7 shows the 3 main fabrics that are distinguished within this rock texture. DD-IIa rhombs are marked by selective dissolution with porosity development along their core/rim interfaces followed by calcite cement infilling the voids inside the rhombs and in the inter-crystalline space (Fig. 8C). The remnants of the original dolomite have a dull red-orange luminescence when viewed under CL. This is well contrasted with the non-luminescent calcite cement (Fig. 8D). DD-IIb shows calcite replacement of the original dolomite rhomb with selective porosity development along the core/rim interface and inside the core (Fig. 8E). The replacing crystals mimic the precursor dolomite microfabrics, i.e. the impure dolomite core is replaced by fine crystalline granular calcite, while the clear outer rims by clear coarser calcite crystals. DD-IIc represents dolomite crystals that are less affected by classical dedolomitization. These crystals show severe structural deformation (e.g. crystal fracturing and fragmentation). Here calcite cement fills the cracks (Fig. 8F). Whether DD-IIc should be included within dedolomite fabrics is debatable. However, the observed corrosion of the dolomite fragments makes them legitimate to be included in the dedolomite fabrics (cf. Budai *et al.*, 1984). The different fabrics of DD-II show a clear dedolomitization trend from the slightly altered dolomite (DD-IIc) to the completely dedolomitized dolomite (DD-IIb), passing by a transitional phase (DD-IIa).

In both types of dedolomites (DD-I and DD-II), the calcite phase (crystallite aggregates and cement) is non-luminescent under CL microscopy, showing a sharp contrast with the dull-luminescent dolomite remnants. The calcite infillings of fractures and veins are also non-luminescent. The non-luminescence suggests calcite precipitation from oxidizing fluids (Barnaby & Rimstedt, 1989). Although the calcite aggregates of DD-Ib generally appear non-luminescent, careful observation suggests minor luminescence zones around the crystallites. This observation is at the limit of the used petrographical techniques, however, its validation may suggest that: 1) dedolomitization have left very tiny dull-luminescent zones of the original dolomitic material in between calcite crystallites, or 2) later calcite (re)crystallization, within more reducing waters, has affected the crystallites. In the case of the second interpretation, sub-oxic to reducing waters might have prevailed in progressively buried dedolomitized rocks deeper than the reach of the surface recharge oxidizing fluids.

6. Geochemistry

Most geochemical data are enumerated in Table 1, which shows the major and trace elemental composition, the $\delta^{13}C$ - $\delta^{18}O$ results, and the dolomite nonstoichiometry ($M\%CaCO_3$) of the various samples. The data are grouped in 7 categories according to their petrographic character-

		Serial #	Sample	Ca	Mg	Sr	Na	Fe	Mn	Zn	K	IR	$d^{18}O$	$d^{13}C$	M% $CaCO_3$
1	Limestone	1	J-1	33,9	0,36	134	164	467	56	51	75	0,8	-5,18	+1.38	-
		2	J-4	32,6	0,29	135	131	156	29	28	31	1,6	-5,40	+1.40	-
		3	J-7	31,8	0,37	186	169	74	20	17	35	2,0	-4,44	+1.42	-
		4	J-9	38,2	0,31	130	111	49	<1	7	29	0,5	-	-	-
		5	JT-3	31,7	0,42	148	150	176	29	24	62	0,2	-3,85	+0.62	-
		6	J-10	32,4	0,33	112	107	43	2	3	57	2,8	-	-	-
		7	J-12	30,9	0,34	180	169	142	<1	3	41	1,0	-	-	-
		8	JT-4	31,5	0,38	125	214	103	22	18	42	2,0	-4,64	+1.83	-
		9	J-19	32,9	0,42	149	201	592	13	7	118	2,3	-	-	-
		10	J-23	33,6	0,34	113	121	139	<1	2	23	0,1	-4,76	+0.15	-
		11	JT-6	32,0	0,52	150	163	224	23	24	84	0,8	-	-	-
		12	J-29-m	32,2	0,50	193	204	531	40	44	137	1,5	-3,84	+1.35	-
		13	JT-7	32,3	0,53	167	122	270	38	4	126	2,0	-3,66	+1.67	-
		14	RB-13	34,7	0,51	297	158	2954	131	13	1086	7,4	-2,65	+1.71	-
		15	JT-8	33,0	0,41	158	162	486	63	15	170	3,5	-2,68	+1.34	-
2	Dedolomite in micrite DD-I	16	J-11	31,8	1,14	120	116	101	20	14	25	1,6	-4,98	+1.15	54,10
3	Dedolomite DD-II	17	J-20	26,3	6,89	53	84	78	19	13	30	1,9	-5,59	-2,32	54,80
		18	JT-5	25,1	7,03	51	115	74	30	16	64	2,5	-5,38	-2,40	53,90
		19	JD-17	-	-	-	-	-	-	-	-	-	-5,16	-2,64	53,83
		20	J-21	32,9	0,50	27	171	41	27	17	37	2,0	-	-	-
		21	J-22	19,5	12,49	75	162	82	34	15	27	2,7	-7,54	+2.12	55,10
4	Dolomite vein	22	J-28-v	19,3	11,46	78	68	9	37	1	11	1,3	-	-	-
		23	J-29-v	19,4	12,20	73	90	27	67	21	19	1,5	-8,37	+2.01	50,94
		24	JT-7-v	18,8	11,22	80	95	19	92	3	28	2,5	-8,72	+2.21	-

		Serial #	Sample	Ca	Mg	Sr	Na	Fe	Mn	Zn	K	IR	$d^{18}O$	$d^{13}C$	M% $CaCO_3$
5	Beige Dolomite	25	J-34	18,4	13,98	20	138	362	41	27	22	1,2	-8,20	+2.27	50,80
		26	RB-0	20,4	13,47	57	112	81	24	7	7	0,7	-8,57	+2.32	49,83
		27	J-36	18,0	13,37	42	258	262	42	23	61	0,1	-	-	-
		28	JT-9	17,7	14,39	42	230	98	36	28	41	0,8	-8,53	+2.41	51,00
		29	JT-S5	17,8	12,80	51	89	104	19	2	19	0,7	-8,18	+2.27	51,67
		30	JT-10	17,7	13,99	39	156	1137	44	24	143	1,2	-	-	-
		31	Z-a	17,1	14,22	46	121	366	51	42	42	0,2	-7,41	+2.39	-
		32	X	17,2	14,04	42	125	88	46	25	43	2,4	-8,30	+2.25	50,60
		33	J-41	17,0	13,82	47	227	60	36	25	39	4,6	-	-	-
		34	J-42	17,3	13,59	40	105	47	44	27	34	2,3	-8,78	+2.27	50,80
		35	J-43	18,5	13,93	36	133	112	45	27	39	1,6	-	-	-
		36	JT-11	19,1	13,95	27	205	811	53	28	98	4,7	-8,25	+2.16	50,40
		37	J-44	19,2	13,96	31	159	352	50	23	78	3,3	-	-	-
		38	J-45	16,1	14,01	27	155	59	40	49	22	3,6	-8,19	+2.24	50,70
6	Gray Dolomite	39	JR-8m	22,3	9,75	104	87	496	63	8	339	2,0	-8,16	+1.94	54,33
		40	J-37	17,7	12,94	78	291	1632	43	35	108	1,5	-	-	53,90
		41	J-38m	17,4	12,76	98	211	599	44	27	250	2,6	-7,82	+2.08	
		42	J-39p	21,7	10,58	101	124	1341	26	7	158	1,1	-8,64	+2.05	54,33
		43	F'	17,6	12,21	140	208	906	46	22	348	3,3	-	-	56,50
		44	D	17,6	12,71	76	192	1729	40	30	396	4,1	-	-	
		45	B	17,9	13,10	78	178	570	44	27	91	1,1	-	-	54,10
		46	JT-S4	18,6	12,63	48	118	609	25	5	181	1,9	-8,76	+2.14	-
		47	JT-S2	18,8	12,10	61	100	1240	51	6	188	2,2	-8,49	+1.90	-
		48	40-mat	17,6	13,44	73	175	1300	48	17	465	3,2	-8,69	+2.25	51,70
		49	Z-b	17,5	12,69	99	172	669	53	27	430	2,9	-7,34	+2.23	52,80
		50	Z-d	17,9	12,88	111	215	1418	46	102	507	2,7	-8,34	+2.20	-
		51	JR-1b	21,7	12,33	74	118	386	44	5	185	2,5	-7,66	+2.24	52,67
		52	Y	17,3	12,31	103	159	1278	46	24	898	4,1	-8,97	+1.97	55,10
7	Spelean calcite vein	53	J-20v	-	-	-	-	-	-	-	-	-	-6,27	-7,00	-
		54	J-34cv	-	-	-	-	-	-	-	-	-	-5,81	-7,43	-
		55	RK-1	-	-	-	-	-	-	-	-	-	-6,21	-9,10	-
		56	J-20s	-	-	-	-	-	-	-	-	-	-4,15	-7,48	-

TABLE 1. Major and trace element composition, $\delta^{13}C$ and $\delta^{18}O$ results, and nonstoichiometry expressed by mole % (M%) $CaCO_3$ of the investigated rock types. Ca and Mg are expressed in wt.% whereas Sr, Na, Fe, Mn and K in ppm. $\delta^{13}C$ and $\delta^{18}O$ in ‰ PDB. "-" is 'not analyzed'.

istics, namely: 1) limestone, 2) partially dedolomitized micrite (DD-I), 3) dedolomite (DD-II), 4) saddle dolomite veins, 5) beige dolomite, 6) gray dolomite and 7) spelean calcite.

Within the DD-I and DD-II categories some further distinctions are worth mentioning. The DD-I values (Tab. 1, group 2) represent bulk-rock analyses of dedolomite rhombs in micritic limestone. In DD-II category, J-22 (typical of DD-IIc fabric; Fig. 5C) shows very slight dedolomitization and is henceforth considered similar to the original precursor dolomite, while J-21 is a completely dedolomitized rock and corresponds to DD-IIb fabric. J-20 and JT-5 have a typical DD-IIa fabric with considerable amounts of both calcite and dolomite phases.

6.1. Major and trace element composition: bulk analyses

56 samples selected along the Daraya tunnel, were used for characterizing the various lithologies with respect to major and trace element composition. Fig. 9 (A, B) shows the resulting Sr to Mg and Fe to K crossplots. The various lithologies exhibit relatively well-defined concentration fields reflecting their distinct elemental compositions. The beige dolomite is characterized by low Sr content (≤ 57 ppm) compared to the gray dolomite (Sr ≥ 48 ppm; Fig. 9A). The minor overlap is mainly due to samples having a transitional nature between both dolomite rock types. In terms of Mg concentration, the former is slightly more enriched than the gray dolomite (by approximately 1 wt.%) which also contains higher mean IR values (insoluble residue, in %). The dedolomitized rocks show a decreasing trend for both Sr and Mg contents. Here, the slightly dedolomitized rocks are characterized by Sr and Mg compositions similar to those of the gray dolomite, whereas the completely dedolomitized rocks have very low concentrations (Mg ~ 0 wt.%; Sr = 26 ppm).

The Fe to K crossplot shows a clear distinction between beige and gray dolomites (Fig. 9B). Both Fe and K contents of the gray dolomite (Fe = 386 to 1729 ppm; K = 91 to 898 ppm) are significantly higher than those of the beige dolomite (Fe = 47 to 366 ppm; K = 7 to 78 ppm). Nevertheless, a few exceptions do occur in both dolomite types. Beige dolomite with a relatively high content of iron-oxides and/or clay minerals in matrix will plot within the field of gray dolomite. The generally higher concentrations of Fe and K in the gray dolomite may be due to higher clay contents compared to the beige counterpart (cf. Swennen *et al.*, 1986). The dedolomite exhibits similar K contents to the beige dolomite (ranging from 27 to 64 ppm), but is somehow less enriched in Fe compared to the latter and to most of the other lithologies (Fe = 41 to 82 ppm).

The beige and gray dolomites have almost the same Na composition. The slightly dedolomitized rock shows similar Na contents to those of the gray dolomite rocks (162 ppm). Further dedolomitization leads to Na depletion. The Na content decrease may imply that dedolomitization occurred under fresh meteoric conditions, as far as the Na concentrations in diagenetic phases can be used to deduce the salinity of the diagenetic fluids (Land, 1980). In conclusion, we can say that the rock diagenetic stabilization is characterized by a depletion in Mg, Sr and Na contents. It is, therefore, likely that meteoric waters were involved in the dedolomitization process (e.g. Brand & Veizer, 1980).

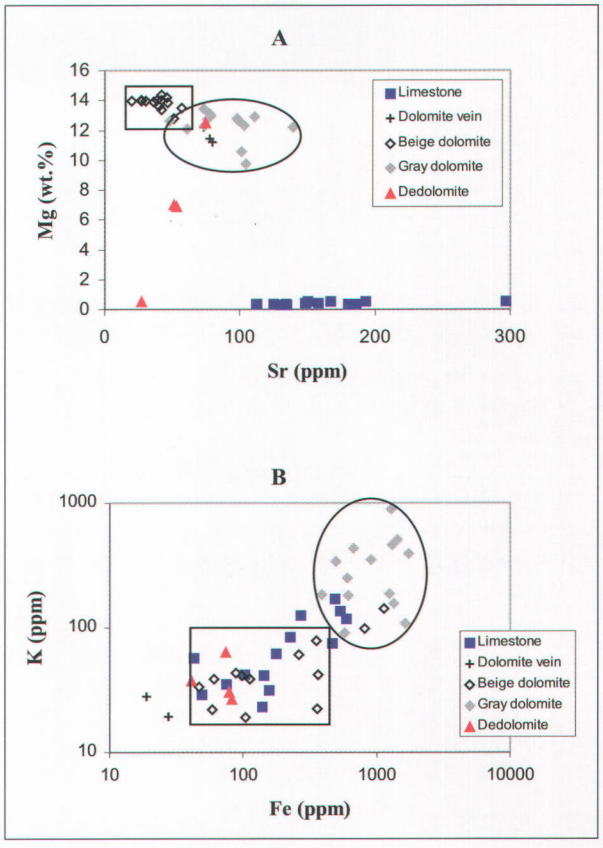

Figure 9. Mg, Sr, Fe and K compositional characteristics of some components of the Kesrouane Formation: (A) Sr (in ppm) versus Mg (in wt.%) crossplot showing a decreasing trend in both elements with increasing dedolomitization, and distinct concentration fields for beige and gray dolomites. (B) Fe versus K (both in ppm) diagram showing a clear concentration distinction between the beige and gray dolomites.

6.2. Major and trace element composition: sequential separation

The above-described results deal with bulk sample analyses. The determination of the chemical characteristics of both original-dolomite and precipitating-calcite phases is a necessity to further unravel the diagenetic conditions during which dedolomitization took place. For this purpose a sequential separation technique was optimized (see methods section) and applied on DD-IIa fabrics where considerable amounts of both phases are preserved. The

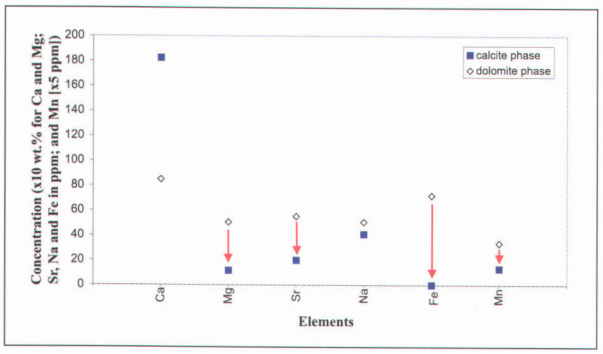

Figure 10. Diagram showing the general chemical characteristics of both dolomite and calcite phases of DD-IIa. The calcite phase exhibits lower concentrations of Mg, Sr, Fe and Mn compared to the original dolomite phase.

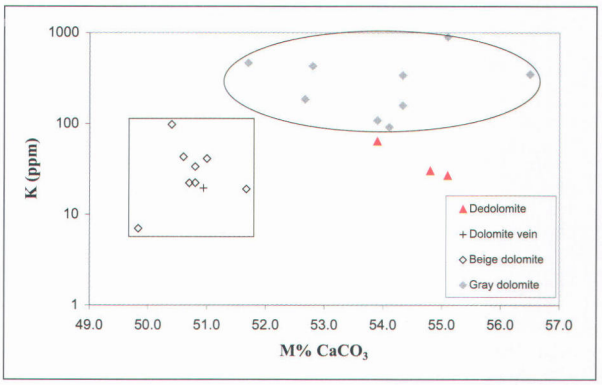

Figure 11. Dolomite nonstoichiometry expressed by mole % (M%) $CaCO_3$ versus K (in ppm) diagram for the major discussed rock types (beige, gray dolomites and dedolomites; values from Table 1). Note that the dedolomites share the same nonstoichiometry of the gray dolomite and similar K concentrations to those of the beige dolomites.

respective Ca, Mg, Na, Fe, Mn and Sr concentrations are shown in Fig. 10. The calcite phase has lower Na, Fe and Sr concentrations compared to the dolomite phase. This suggests, as concluded before, that dedolomitization released these elements into the solution, rather than incorporated ions of these elements into the calcite-phase.

Surprisingly, Fe is absent in the calcite phase. Considering the Fe content of the original dolomite rocks (ca. 82 ppm), we are faced with the inevitable question: is Fe liberated during dedolomitization? If the dedolomitization occurred in a closed system with respect to Fe, we would expect the latter to be included in the calcite or into other Fe-bearing phases. Since no significant Fe-bearing phases were found within the dedolomitized zones, the problem remains unsolved.

6.3. Dolomite stoichiometry

According to Lumsden and Chimahusky (1980), dolomite nonstoichiometry, expressed as mole percent (M%) $CaCO_3$, seems not to be related to most of the petrographic parameters (e.g. insoluble residue, porosity, rock-type, fossil component and dolomite crystal size). Nevertheless, the stoichiometry gives an idea about the original identity of the dolomite and its stability (e.g. Sperber *et al.*, 1984). Less stable nonstoichiometric dolomite have an intrinsic thermodynamic drive for alteration to more stable stoichiometric dolomite (Carpenter, 1980; Land, 1980). The most stable dolomite crystals have a nonstoichiometry ranging between 50.0 and 52.0 M% $CaCO_3$, while less stable crystals range from 49.0 to 50.0, and 52.0 to 58.0 M% $CaCO_3$ (Lumsden & Chimahusky, 1980). According to Dorobek et al. (1993), the readiness of the dolomite crystals to be altered is partially controlled by their nonstoichiometry; this may also be the case for dedolomitization.

The beige dolomite rocks are characterized by a nonstoichiometry ranging between 49.8 and 51.7 M% $CaCO_3$ (see Table 1). These dolomites can be considered as nearly stoichiometric. The gray dolomite rocks have nonstoichiometry values between 51.7 and 56.5 M% $CaCO_3$, hence, they are believed to be less stable. All the investigated dedolomite fabrics, except DD-IIc, which is completely dedolomitized, resulted in similar nonstoichiometry values of the remaining dolomite ranging between 53.8 and 55.1 M% $CaCO_3$ (Fig. 11).

6.4. Carbon and oxygen stable isotopes

The results of the carbon and oxygen isotopic composition of the Daraya sequence are shown in Fig. 12. Since the oxygen and carbon isotopic composition of the sea water shows some variation through geologic time (Qing *et al.*, 2001), it is necessary to estimate the initial composition of the Early Jurassic marine carbonate as a starting isotopic signature. Accordingly, the $\delta^{13}C$ and $\delta^{18}O$ values of calcite precipitated from Early Jurassic seawater are from +1‰ to +4‰ PDB and -3‰ to -1‰ PDB, respectively (Qing *et al.*, 2001).

The analyzed micritic limestone and dolomite define relatively wide $\delta^{18}O$ compositional ranges (limestone: -2.65‰ to -5.40‰; dolomite: -7.34‰ to -8.97‰), while the $\delta^{13}C$ values lie in a narrow range similar to the original marine signature. The relatively wide range of $\delta^{18}O$ values may suggest multiple-step recrystallization of the limestone and dolomite (Nielsen *et al.*, 1994). Within the limestone field, the slight $\delta^{13}C$ values decrease with respect to the original marine signature could be related to meteoric diagenesis.

The investigated dedolomite rocks define a narrow compositional field with isotope values ranging from -5.16 to -5.59‰ $\delta^{18}O$ and -2.32 to -2.64‰ $\delta^{13}C$. These values represent bulk-rock analyses, and are significantly lower than the isotopic composition of the original marine carbonate. Telogenetic spelean calcite, occurring as void infilling in pre-existing dolomite veins within the replace-

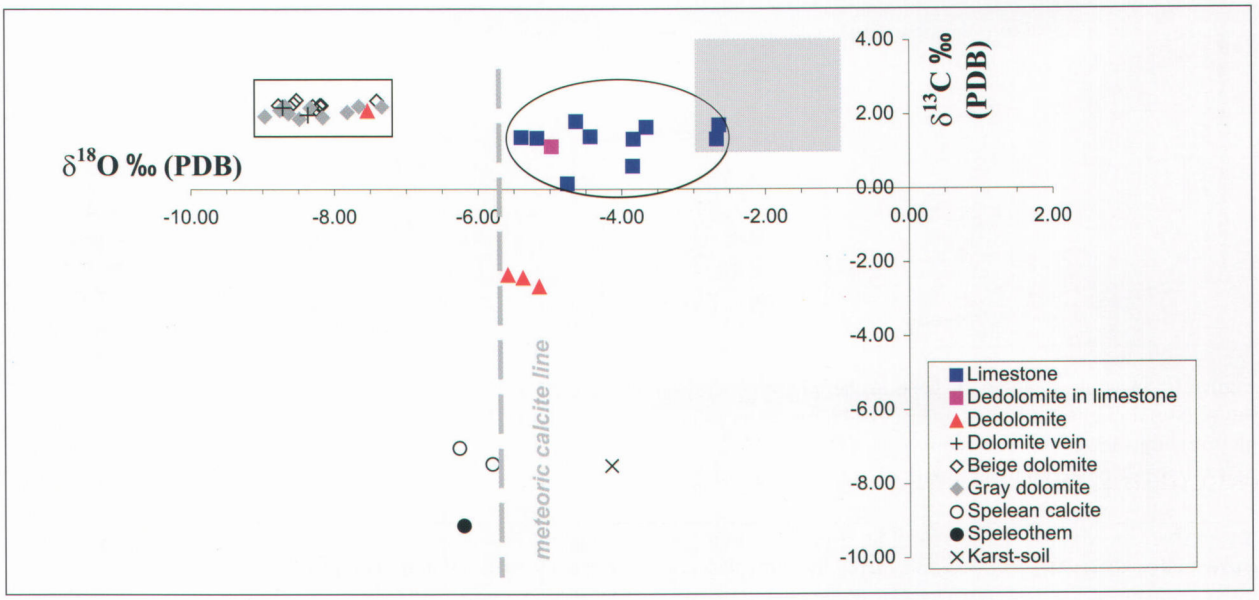

Figure 12. Carbon and Oxygen isotopic compositions of the Kesrouane Formation constituents. The gray square represents the Jurassic marine signature (from Qing *et al.* 2001).

ment beige dolomites and dedolomite pockets, resulted in very depleted $\delta^{13}C$ values ranging between -7.00 and -7.43‰, with $\delta^{18}O$ values between -5.81 and -6.27‰. Recent speleothem (formed after the construction of the tunnel in 1971) resulted in almost a similar $\delta^{18}O$ value (-6.21‰) and more depleted $\delta^{13}C$ (-9.10‰). The dedolomite, the spelean calcite, and the recent speleothems have almost the same $\delta^{18}O$ signature. This coincides with the lowest $\delta^{18}O$ values of the limestone within the investigated sequence. Highly variable (depleted) $\delta^{13}C$ coupled with relatively invariant $\delta^{18}O$ characterize fresh meteoric environments (Allan & Matthews, 1982; Lohmann, 1988), although it can be interpreted also in other ways (e.g. burial diagenesis with hydrocarbon maturation defined by Budai *et al.*, 1984). The 'meteoric calcite line' represents a trend of karst-meteoric alteration of the original limestone and dolomite by means of surface fluids rich in soil derived $\delta^{13}C$. According to Lohmann (1988), this line also delineates the $\delta^{18}O$ of the diagenetic fluid.

7. Discussion

The different dedolomite fabrics are the product of the reaction between precursor rocks and dedolomitizing fluids. Thus, any petrographic description scheme should start with classifying the dedolomite rocks according to the lithology of their original rocks. Then, two main factors seem to control the resulting fabrics, the degree and mode of dolomitization and subsequent dedolomitization. In the present study, two dedolomite types, produced from two different lithologies, are discussed (DD-I originating from a partially dolomitized micritic limestone, and DD-II from a completely dolomitized rock). Partial or complete dedolomitization may lead to different fabrics (DD-Ia, DD-IIa; and DD-Ib, DDIIb respectively). The mode of dedolomitization may fashion the resulting fabrics. For instance, within the fabrics of DD-I, we can distinguish the selective from the nonselective dedolomitization (DD-Ia and DD-Ib, respectively). This selectivity also affects DD-II, where dedolomite end-product might be a mimic replica of the original dolomite (DD-IIb).

The $\delta^{13}C$ and $\delta^{18}O$ composition of the dedolomite suggest that the dedolomitizing fluids were karst meteoric waters. The decrease in $\delta^{13}C$ values with respect to the original marine carbon signature is explained by the involvement of soil derived $\delta^{13}C$. This conclusion fits with the field observation of paleokarst features associated to the dedolomitized rock exposures. The non-luminescent CL pattern of the calcite aggregates and cements (product of the dedolomitizing fluids) suggests also that these waters were oxidizing. As mentioned above, the 'meteoric calcite line' ($\delta^{18}O$ values between -6.0 and -5.0‰PDB) may be used in order to estimate the $\delta^{18}O$ composition of the calcitizing fluids. The graphical method of Woronick & Land (1985) was followed for this purpose (Fig. 13). Consequently, for modeled temperatures ranging between 10 and 20°C (known temperature for caves in Jiita), the original $\delta^{18}O$ composition of the meteoric fluids is estimated to range from -3.8 to -7.2‰ SMOW.

The selective analysis of the calcite and dolomite phases from dedolomitized rocks resulted in chemical characterization of the remnant dolomite representing the precursor rocks and the calcite that is related to the

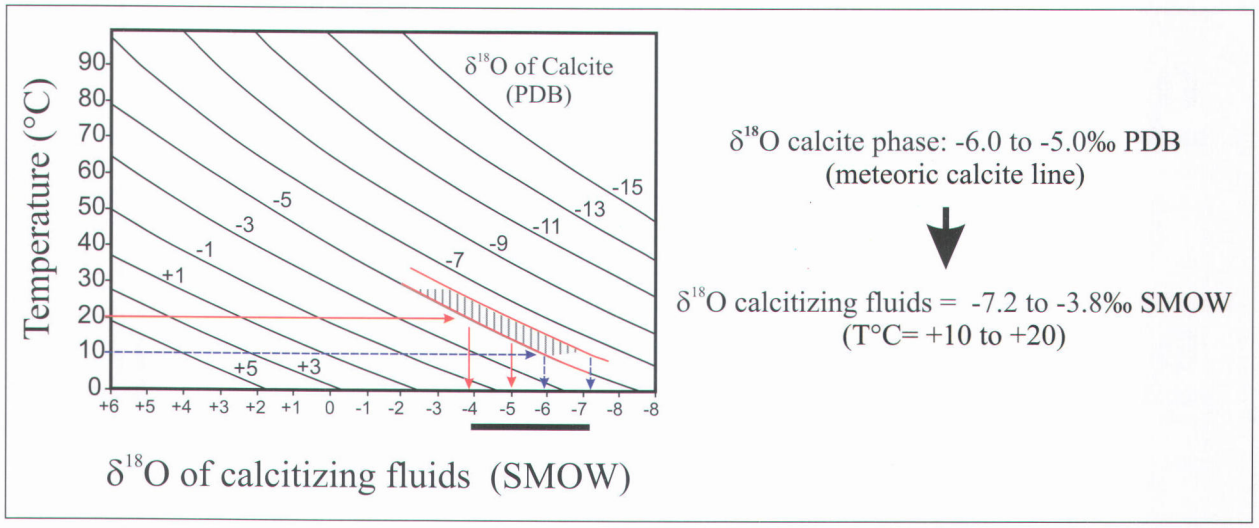

Figure 13. Graphical display of the oxygen isotopic equilibrium relationship between water, temperature of precipitation and calcite minerals (Woronick & Land, 1985). Estimation of the $\delta^{18}O$ composition of the calcitizing waters for modeled temperatures between 10 and 20°C.

dedolomitizing fluids. It also confirmed the conclusions deduced from bulk analysis. Hence, Mg, Sr, Na, and Fe were released from the precursor dolomite into the solution during dedolomitization. But, the precipitating calcite did not incorporate these elements.

By analogy to the aragonite-calcite transformation (cf. Pingitore, 1978), the main factors controlling the trace and minor element distribution in cogenetic calcite precipitation during dedolomitization are: 1) the chemistry of the original dolomite, 2) the partitioning coefficients for the ionic trace elements at specific temperatures, 3) the chemistry of the diagenetic fluid before entering the system, 4) the flow system (open / closed), and 5) the non-carbonate chemical reactions. According to Pingitore (1978), the relative depletion or enrichment of the produced calcite in a certain trace element compared to the original rock can be modeled once the first four variables are known. For instance, Fe, which has a partitioning coefficient ranging between 1 and 50 (i.e. ≥ 1; Janssen, 2000) may be depleted in the precipitating calcite if the initial diagenetic fluid has lower Fe concentrations compared to the original dolomite and when the flow system is open. From another point of view, reducing conditions are generally necessary for Fe cations to be incorporated into the carbonate lattice (Humphrey, 1988; Lohmann, 1988). Thus, the observed lack of Fe in the calcite phase may be explained by the existence of an open system where fluids were oxidized and less enriched in Fe compared to the dedolomitized rocks. For the case of Na, the proposal of dedolomitization by means of fresh waters might be an adequate argument for its low concentrations in the produced calcite.

In meteoric environments, Mg and Sr cations in solution are believed to originate mainly from the pre-existing mineral phases (Lohmann, 1988). An open system may provide one explanation for the non-incorporation of the released Sr cations in the precipitating calcite, even if the initial fluids have Sr concentrations slightly equal or greater than that of the original dolomite (Pingitore, 1978). Fig. 9A shows a clear Mg and Sr depletion with increasing dedolomitization. The gray dolomites and the remaining dolomitic phases in dedolomites share a similar nonstoichiometry compared to that of the near stoichiometric beige dolomites.

As we have mentioned before, paleo- and recent karst features are present randomly within the various lithological zones intercepted by the Daraya tunnel. The dolomite recrystallization implies alteration to more stoichiometric states and crystalline stability. Therefore, the nearly stoichiometric beige dolomites are not affected by dedolomitization (whether paleo- and/or recent karst features are present). Meteoric calcite cement is observed only in intercrystalline pores within the beige dolomite matrix. The insoluble residues (IR%), Fe and K concentrations of both beige and gray dolomites favor the proposal of a relationship between clay contents and dolomite nonstoichiometry in the investigated sequence. The clays seem to have prohibited the ideal (re)crystallization of gray dolomites (probably by decreasing the rock permeability not allowing the circulation of diagenetic fluids). As dolomite (re)crystallization usually leads to more stoichiometric and ordered crystals, the gray dolomites remained nonstoichiometric. Similarly, the high clay content may have played a major role in protecting these dolomites from dedolomitization (Fig. 11).

Dedolomitization appears to be restricted to the dolomite pockets that are located within the micritic limestone rock-mass. These pockets are made up of dolomites that

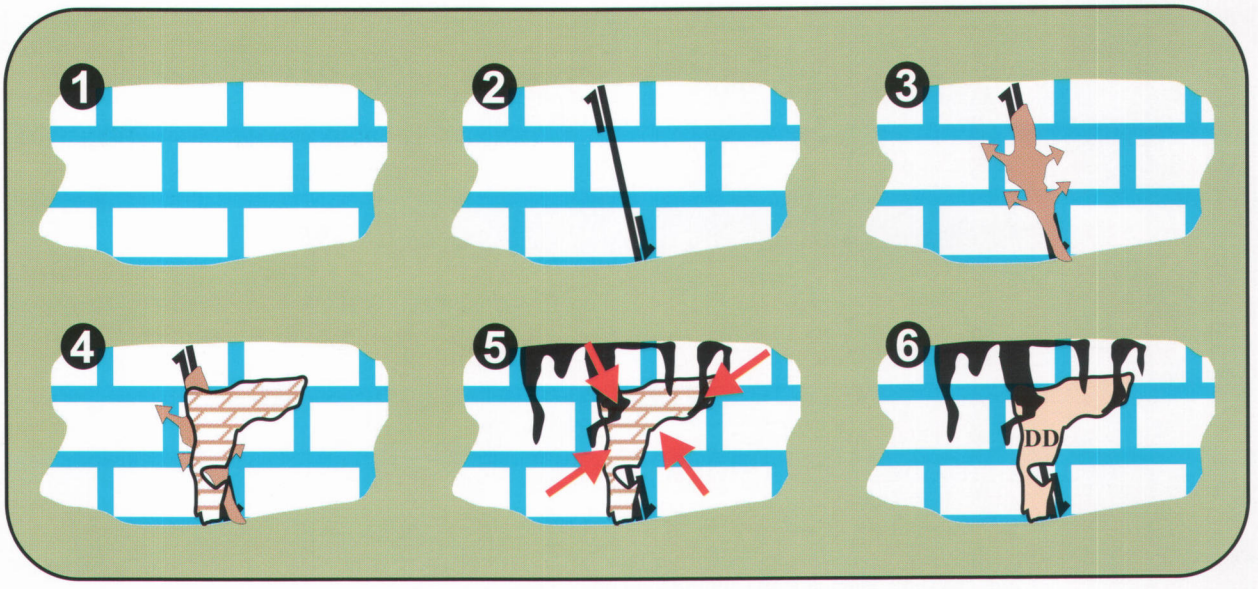

Figure 14. Graphical illustration of the concept of dolomite/dedolomite pockets: 1. Micritic limestone, 2. Faulting/fracturing, 3. Dolomitizing fluids circulation along faults, 4. Dolomitization of limestone surrounding the premises of fluid flow (dolomite pocket), 5. Relative increase of porosity and permeability inside the dolomite pocket compared to the surrounding limestone; upon emergence and karstification, the dolomite pocket becomes a preferential conduit horizon for meteoric waters, and 6. Dedolomitization inside the pocket.

are nonstoichiometric (similar to the gray dolomite), but with petrographic and geochemical traits similar to those of the hydrothermal beige dolomites. Fig. 14 describes the proposed stages of evolution of these pockets. Local dolomitization within the limestone occurred through the hydrothermal fluid activity along faults and/or fractures similarly to the beige dolomite. This led to the creation of higher permeability gradient with respect to the surrounding mudstone-wackestone due to the higher intercrystalline porosity of dolomites. After emergence and karstification, the dolomite pockets became preferential zones for the circulation of meteoric calcitizing fluids and subsequent dedolomitization. No unequivocal arguments are presently known in order to determine whether this dedolomitization occurred during the early emergence of northern Mount-Lebanon in the Late-Jurassic times, or as a consequence of the final Neogene uplift of the Lebanese mountain chains.

The present case shows that careful dedolomite inspection helps to unravel useful information about dedolomitization and related processes (e.g. dissolution, cementation). The remaining dedolomite phases hold the imprints of the diagenetic conditions (e.g. uplift, emergence and karstification), that prevailed at the time of dedolomitization. Moreover, these phases may serve to comprehensively assess the dynamic nature of the system flow in paleokarst.

8. Summary and Conclusions

In summary, based on petrographic and geochemical data of the Lower Jurassic dolomites and dedolomites of central Lebanon (Kesrouane Formation), the following points can be concluded:

1. The dedolomite fabrics are controlled primarily by the lithology of the original rock. A scheme for petrographic classification is proposed based on the original rock texture, the degree and mode of dedolomitization.

2. The dedolomitization of the investigated Jurassic carbonates occurred as a result of the migration of karst-related meteoric waters into previously dolomitized pockets within the limestone rock-mass, during a period of emergence which age could be Late Jurassic (corresponding to the early uplift of northern Lebanon) or Neogene (upon the final uplift of the Lebanese mountain ranges). Since the dedolomitizing fluids are believed to be fresh oxidizing waters in an open system, Mg, Sr, Na and Fe were released from the pre-existing dolomite minerals into the solution without being incorporated in the precipitating calcite.

3. Dolomite stoichiometry of the original rock appears to play an important role in controlling dedolomi-

tization, which, in the present case, is restricted to the less stable nonstoichiometric dolomite.

4. The relatively high clay contents of the gray dolomites may have prohibited ideal (re)crystallization, and subsequent resetting to more enhanced stoichiometric states. This may have also protected them from dedolomitization, although their nonstoichiometry is similar to that of the remaining dolomite pahses in the dedolomites.

5. The proper petrographic and geochemical investigation of dedolomites provides a remarkable tool for learning something about the diagenetic conditions that occurred during dedolomitization - in the present case, these conditions are related to emergence and karstification. In other words, the followed approach may be reversed leading to the determination and assessment of paleokarst flow systems from the inspection of dedolomites.

9. Acknowledgements

The authors are grateful to Dr. S. Verheyden for reviewing the manuscript. Dr. M. Joachimski is thanked for performing the isotopic analyses. D. Coetermans and H. Nijs are also acknowledged for the technical assistance. This work is partially sponsored by the Katholieke Universiteit Leuven (Afd. Fysico-chemische geologie). The first author (F. Nader) benefited of a research grant from the Lebanese National Council for Scientific Research. Critical reviews and valuable comments made by Dr. A. Préat and Dr. M. Hennebert have improved the presentation and content of this contribution, and are greatly appreciated.

10. References

ABU-SHUSHAH, M. K. A., 1976. *Petrography of some Cretaceous sediments from Lebanon (Aptian - Albian - Cenomanian of the Bhamdoun region)*. M.S. thesis, American University of Beirut, Beirut, Lebanon, 92 p.

ABDEL-RAHMAN, A.-F. M. & NADER, F. H., 2002. Characterization of the Lebanese Jurassic-Cretaceous carbonate stratigraphic sequence: a geochemical approach. *Geological Journal*, 37, 69-91.

AL-HASHIMI, W. S. & HEMINGWAY, J. E., 1973. Recent dedolomitization and the origin of the rusty crusts of Northumberland. *Journal of Sedimentary Petrolology*, 43 (1), 82-91.

ALLAN, J. R. & MATTHEWS, R. K., 1982. Isotope signatures associated with early meteoric diagenesis. *Sedimentology*, 29, 797-817.

BACK, W., HANSHAW , B. B., PLUMMER, L. N., RAHN, P. H., RIGHTMIRE, C. T. & RUBIN, M., 1983. Process and rate of dedolomitization: mass transfer and ^{14}C dating in a regional carbonate aquifer. *Geological Society of America Bulletin*, 94, 1415-1429.

BARNABY, R. J. & RIMSTEDT, J. D., 1989. Redox conditions of calcite cementation interpreted from Mn and Fe contents of authigenic calcites. *Geological Society of America Bulletin*, 101, 795-804.

BEYDOUN, Z. R., 1988. *The Middle-East: Regional geology and petroleum resources*. Scientific Press, London, 292 p.

BRAND, U. & VEIZER, J., 1980. Chemical diagenesis of a multicomponent carbonate system – I: Trace elements. *Journal of Sedimentary Petrology*, 50, 1219-1236.

BRAUN, M. & FRIEDMAN, G. M., 1970. Dedolomitization fabric in peels: a possible clue to uncomformity surfaces. *Journal of Sedimentary Petrology*, 40, 417-419.

BREW, G., BARAZANGI, M., AL-MALEH, A. K. & SAWAF, T., 2001. Tectonic and geologic evolution of Syria. *GeoArabia*, 6 (4), 573-615.

BUCHBINDER, L. G., 1981. Dolomitization, porosity development and late mineralization in the Jurassic Zohar (Brur calcarenite) and Sederot Formations in Ashdod-Gan Yavne. *Israel Journal of Earth-Sciences*, 30, 64-80.

BUDAI, J. M., LOHMANN, K. C. & OWEN, R. M., 1984. Burial dedolomitization in the Mississippian Madison Limestone, Wyoming and Utah Thrust Belt. *Journal of Sedimentary Petrology*, 54 (1), 0276-0288.

BURNS, S. J. & BAKER, P. A., 1987. A geochemical study of dolomite in the Monterey Formation, California. *Journal of Sedimentary Petrology*, 57 (1), 128-139.

BUTLER, R. W. H., SPENCER, S. & GRIFFITHS, H. M., 1997. Transcurrent fault activity on the Dead Sea Transform in Lebanon and its implications for plate tectonics and seismic hazard. *Journal of the Geological Society, London*, 154, 757-760.

BUTLER, R. W. H., SPENCER, S. & GRIFFITHS, H. M., 1998. The structural response to evolving plate kinematics during transpression: evolution of the Lebanese restraining bend of the Dead Sea Transform. In Holdsworth, R. E., Strachan, R. A. & Dewey, J. F., eds., Continental Transpressional and Transtensional Tectonics. *Journal of the Geological Society, London*. Special Publications, 135, 81-106.

BUTLER, R. W. H. & SPENCER, S., 1999. Landscape evolution and the preservation of tectonic landforms along the northern Yammouneh Fault, Lebanon. *Journal of the Geological Society, London*. Special Publications, 162, 1-14.

CARPENTER, A. B., 1980. The chemistry of dolomite formation I: The stability of dolomite. *Special Publications of the Society of Economical Paleontology Mineralogists*, Tulsa, 111-121.

DOROBEK, S. L., SMITH, T. M. & WHITSITT, P. M., 1993. Microfabrics and geochemistry of meteorically altered dolomite in Devonian and Mississipian carbonated, Montana and Idaho. In Rezak, R. & Lavoie, D. L., eds., *Carbonate Microfabrics*. Springer-Verlag, New York, 205-225.

DUBERTRET, L., 1955. *Carte géologique du Liban au 1/200000 avec notice explicative*. République Libanaise, Ministère des Travaux Publiques, Beirut, 74 p.

EVAMY, B. D., 1963. The application of a chemical staining technique to a study of dedolomitization. *Sedimentology*, 2, 164-170.

EVAMY, B. D., 1967. Dedolomitization and the development of rhombohedral pores in limestones. *Journal of Sedimentary Petrology*, 37, 1204-1215.

FOLKMAN, Y., 1969. Diagenetic dedolomitization in the Albian-Cenomanian Yagur Dolomite on Mount Carmel (Northern Israel). *Journal of Sedimentary Petrology*, 39, 380-385.

GOLDBERG, M., 1967. Supratidal dolomitization and dedolomitization in Jurassic rocks of Hamakhtesh Hagatan, Israel. *Journal of Sedimentary Petrology*, 37, 760-773.

GOLDBERG, M. & BOGOCH, R., 1978. Dolomitization and hydrothermal mineralization in the Brur Calcarenite (Jurassic), southern Coastal Plain, Israel. *Israel Journal of Earth-Sciences*, 27, 36-41.

GOLDSMITH, J. R. & GRAF, D. L., 1958. Relations between lattice constants and composition of Ca-Mg carbonates. *American Mineralogist*, 43, 84-101.

GOMEZ, F., MEGHRAOUI, M., DARKAL, A. N., SBEINATI, R., DARAWCHEH, R., TABET, C., KHAWLIE, M., CHARABE, M., KHAIR, K. & BARAZANGI, M., 2001. Coseismic displacements along the Serghaya Fault: An active branch of the Dead Sea Fault System in Syria and Lebanon. *Journal of the Geological Society, London*, 158, 1-4.

GRIFFITHS, H. M., CLARK, R. A., THORP, K. M. & SPENCER, S., 2000. Strain accommodation at the lateral margin of an active transpressive zone; geological and seismological evidence from the Lebanese restraining bend. *Journal of the Geological Society, London*, 157, 45-68.

GROVER, G. I. & READ, J. R., 1983. Paleoaquifer and deep burial cements defined by cathodoluminescent patterns, Middle Ordovician carbonates. *American Association of Petroleum Geologists Bulletin*, 67, 1275-1303.

HUMPHREY, J. D., 1988. Late Pleistocene mixing zone dolomitization, southern Barbados, West Indies. *Sedimentology*, 35, 327-348.

JANSSEN, A., 2000. *Petrography and geochemistry of active and fossil tufa deposits from Belgium*. Ph.D. thesis Katholieke Universiteit Leuven, Leuven, Belgium, 392 p.

JA'OUNI, A. K., 1971. *Stratigraphy of north-central Lebanon*. M.S. thesis American University of Beirut, Beirut, Lebanon, 114 p.

KATZ, A., 1968. Calcian dedolomite and dedolomitization. *Nature*, 217, 439-440.

KATZ, A., 1971. Zoned dolomite crystals. *Journal of Geology*, 79, 38-51.

KYUNG, W. S. & MOORE, C. H., 1996. Burial dolomitization and dedolomitization of the Late Cambrian Wagok Formation, Yeongweol, Korea. *Carbonates and Evaporites*, 11 (2), 104-112.

LAND, L. S., 1980. The isotopic and trace element geochemistry of dolomite: The state of the art. In Zenger, D. H., Dunham, J. B. & Ethington, R. L., eds., Concepts and Models of Dolomitization. *Special Publications of the Society of Economical Paleontology Mineralogists*, Tulsa, 28, 87-110.

LAND, L. S. & PREZBINDOWSKI, D. R., 1981. The origin and evolution of saline formation waters, lower Cretaceous carbonates, south-central Texas, U.S.A. *Journal of Hydrology*, 54, 51-74.

LOHMANN, K. C., 1988. Geochemical patterns of meteoric diagenetic systems and their application to studies of paleokarst. In James, N. P. & Choquette, P. W., eds., *Paleokarst*. Springer-Verlag, New York, 58-80.

LONGMAN, M. W. & MENCH, P. A., 1978. Diagenesis of Cretaceous carbonates in the Edwards aquifer system south-central Texas: a scanning electron microscope study. *Sedimentary Geology*, 21, 241-271.

LUMSDEN, D. N., 1979. Discrepancy between thin section and X-ray estimates of dolomite in limestone. *Journal of Sedimentary Petrology*, 49, 429-436.

LUMSDEN, D. N. & CHIMAHUSKY, J. S., 1980. Relationship between dolomite nonstoichiometry and carbonate facies parameters. *Special Publications of the Society of Economical Paleontology Mineralogists*, Tulsa, 28, 123-137.

MACHEL, H. G., 2000. Application of cathodoluminescence to carbonate diagenesis. In Pagel, M., Barbin, V., Blanc, P. & Ohnenstetter, D., eds., *Cathodoluminescence in Geosciences*. Springer-Verlag, Berlin Heidelberg, 271-301.

MAGARITZ, M. & KAFRI, U., 1981. Stable isotope and Sr^{2+}/Ca^{2+} evidence of diagenetic dedolomitization in a schizohaline environment: Cenomanian of northern Israel. *Sedimentary Geology*, 28, 29-41.

NIELSEN, P., SWENNEN, R. & KEPPENS, E., 1994. Multiple-step recrystallization within massive ancient dolomite units: an example from the Dinantian of Belgium. *Sedimentology*, 41, 567-584.

NOUJEIM, G., 1977. *Pétrographie et environnements sédimentaires de l'Albien, Cénomanien, Turonien dans les environs Nord de Beyrouth (Liban)*. Diplôme de Docteur 3° cycle à l'Université Pierre et Marie Curie, Paris 6, 157 p.

PINGITORE, N. E., 1978. The behavior of Zn^{2+} and Mn^{2+} during carbonate diagenesis: Theory and applications. *Journal of Sedimentary Petrology*, 48 (1), 799-814.

QING, H., BOSENCE, D. W. & ROSE, E. P. F., 2001. Dolomitization by penesaline sea water in Early Jurassic peritidal platform carbonates, Gibraltar, western Mediterranean. *Sedimentology*, 48, 153-163.

RENOUARD, G., 1951. Sur la découverte du Jurassique inférieur (?) et du Jurassique Moyen au Liban. *Comptes Rendues Académie des Sciences*, 232, 992-994.

RENOUARD, G., 1955. Oil Prospects of Lebanon. *American Association of Petroleum Geologists Bulletin*, 39 (11), 2125-2169.

RONCHI, P., LOTTAROLI, F., RICCHIUTO, T., 2000. Sedimentary and diagenetic aspects of the Liassic Inici Fm and its stratigraphic context (Sicily Channel, Italy). *Memoria Societa Geologica Italiana*, 55, 261-269.

ROSENBAUM, J. & SHEPPARD, S. M., 1986. An isotopic study of siderites, dolomites and ankerites at high temperatures. *Geochimica Cosmochimica Acta*, 50, 1147-1150.

SAINT-MARC, P., 1974. Etude stratigraphique et micropaléontologique de l'Albien, du Cénomanien et du Turonien [in "*Note et mémoires sur le Moyen-Orient – Tome XIII*"]. CNRS, Paris-Beirut, 342 p.

SAINT-MARC, P., 1980. Le passage Jurassique-Crétacé et le Crétacé inférieur de la région de Ghazir (Liban central). *Géologie Méditerranéenne*, VII, 237-245.

SEARL, A., 1989. Saddle dolomite: a new view of its nature and origin. *Mineralogical Magazine*, 53, 547-555.

SEBER, D., VALLVE, M., SANDVOL, E., STEER, D. and BARAZANGI, M., 1997. Middle-East Tectonics: Applications of Geographic Information Systems (GIS). *GSA Today*, 7 (2), 1-6.

SIBLEY, D. F. & GREGG, J. M., 1987. Classification of dolomite rock textures. *Journal of Sedimentary Petrology*, 57, 967-975.

SPERBER, C. M., WILKINSON, B. H. & PEACOR, D. R., 1984. Rock composition, dolomite stoichiometry, and rock/water reactions in dolomitic carbonate rocks. *Journal of Geology*, 92 (6), 609-622.

SWENNEN, R., VIAENE, W., BOUCKAERT, J., SIMAKOV, K. V. & VAN OYEN, P., 1986. Lithogeochemistry of Upper Famennian-Tournaisian strata in the Omolon area (NE-USSR) and its implications. *Annales de la Société Géologique de Belgique*, 109, 249-261.

WACHTER, E. & HAYES, J. M., 1985. Exchange of oxygen isotopes in carbon-dioxide – phosphoric acid systems. *Chemical Geology*, 52, 365-374.

WALLEY, C. D., 1983. A revision of the Lower Cretaceous stratigraphy of Lebanon. *Geologische Rundschau*, 72, 377-388.

WALLEY, C. D., 1997. The Lithostratigraphy of Lebanon: A Review. *Lebanese Scientific Research Reports*, 10 (1), 81-108.

WORONICK, R. E. & LAND, L. S., 1985. Late burial diagenesis, Lower Cretaceous Pearsall and Lower Glen Rose formations, South Texas. In Schneidermann, N. & Harris, P. M., eds., *Carbonate Cements. Special Publications of the Society of Economical Paleontology Mineralogists*, Tulsa,, 36, 265-275.

Manuscript received 01.03.02. and accepted for publication 01.07.02.